



ISSN: 0067-2904

Synthesis , Physicochemical Identification With Antimicrobial And Anti-inflammatory Evaluation of Some New Metal Complexes Derived From Enprofylline

Alyaa Khider Abbas^{1*}, Noor Adel Hussein^{2*}, Asmaa Mohammed Noori Khaleel^{1*}

¹Department Of Chemistry, College Of Science, University Of Baghdad, Baghdad, Iraq

²Department Of Chemistry , College Of Science, Al-Mustansiriyah University, Baghdad, Iraq

Received: 1/2/2025

Accepted: 29/5/2025

Published: 30/5/2026

Abstract:

This study outlines the synthesis of the ligand [(4-((2,6-dioxo-3-propyl-2,3,4,5,6,7-hexahydro-1H-purin-8-yl) BAE] through a diazo coupling reaction between enprofylline and 4-amino-2-chlorobenzaldehyde. This ligand was then complexed with Co(II), Cu(II), Pd(II), Ag(I) and Pt(IV). The molecular structures of the resulting complexes were characterized using spectral including thermal and physicochemical techniques. The complexes exhibit a (1:2)(M:L) stoichiometry .The FTIR study corroborated that BAE ligand acts as neutral N,N-bidentate and chelated with selected metal ions via(N-9) atom of imine group in imidazole and nitrogen atom of azo group and they yield tetrahedral geometry for Ag-BAE, square planar for Pd-BAE and octahedral for the remained complexes. All synthesized compounds demonstrated high thermogravimetric analysis (TGA) studies. Additionally, the calculated stability constant and ΔG of complexes confirmed the thermodynamic stability and spontaneous reaction . The BAE ligand and its complexes exhibit good antibacterial activity against two types of selected bacteria, when compared with amoxicillin drug as standard. The antioxidant ability of Cu-BAE and Pt-BAE complexes were examined by utilizing reductive activity and DPPH radical scavenging with Trolox and ascorbic acid as standard respectively ,the data indicate significant antioxidant activity. The(Pd-BAE)complex exhibited strong anti-inflammatory in wound healing assessments, showing significant effectiveness in treating burns and wounds ,which is took(9) days to heal, while the silver sulfadiazine drug as standard has (16) days and without treatment(18) days .Finally, the cytotoxic effectiveness of (Co-BAE) complex against the colon cancer cell line CaCo₂ was investigated using MTT assay, revealing potential as an anticancer agent with IC₅₀ 109.1 mg ml⁻¹ when compared with the normal cell line (WRL68) .

Keywords: Enprofylline, Azo-ligand, spectral studies ,anti-inflammatory, antioxidant, anticancer.

تحضير وتشخيص فيزيوكيميائي مع تقييم مضاد الميكروبات ومضاد الالتهاب لبعض المعقدات الفلزية المشتقة من انبروفيلين

علياء خضر عباس^{1*} ، نور عادل حسين^{2*} ، اسماء محمد نوري خليل^{1*}

¹ قسم الكيمياء ، كلية العلوم ، جامعة بغداد ، بغداد ، العراق

² قسم الكيمياء ، كلية العلوم ، الجامعة المستنصرية ، بغداد ، العراق

*Email: nooraadil23@uomustansiriyah.edu.iq

الخلاصة

تتناول هذه الدراسة تحضير الليكاند [(4) - (2,6-دايوكسو-3-بروبيل-2,4,5,6-هيكساهيدرو-1H-بيورين-8-يل) BAE] من خلال تفاعل اقتران ثنائي الأزو بين الانبروفيلين و4-امينو-2-كلورونينزالديهايد . بعد ذلك تم تكوين معقدات لهذه الليكاند مع (Co(II) و Cu(II) و Pd(II) و Ag(I) و Pt(IV). الأشكال الجزيئية للمعقدات الناتجة سُخِصت باستخدام التقنيات الطيفية بما في ذلك الحرارية والفيزيوكيميائية . المعقدات أظهرت النسبة الكيميائية (2:1) (فلز : ليكاند). أكدت دراسة FTIR ان الليكاند BAE يعمل كثنائي سن N,N متعادل ويرتبط مخلبياً بأيونات فلزية مختارة عبر ذرة N-9 لمجموعة الامين في الاميدازول وذرة نتروجين لمجموعة الأزو واعطت شكل هندسي رباعي سطوح لـ Ag-BAE ومربع مستوي لـ Pd-BAE وثمانى سطوح للمعقدات المتبقية . أظهرت دراسات TGA ان جميع المركبات المحضرة لها تحليل وزني حراري عالي . بالإضافة الى ذلك ، فان ثابت الاستقرار و ΔG المحسوبة للمعقدات اثبتت الاستقرارية الثرموديناميكية والتفاعل التلقائي . الليكاند BAE ومعقداتها أظهرت فعالية جيدة كعوامل مضادة للبكتيريا ضد نوعين مختارة من البكتيريا مقارنة بدواء الاموكسيسيلين كمعيار . تم فحص قدرة مضادات الاكسدة للمعقدات Cu-BAE و Pt-BAE من خلال استخدام النشاط الاختزالي وازالة الجذور الحرة DPPH باستخدام Trolox وحامض الاسكوربيك كمعيار على التوالي ، اشارت النتائج الى فعالية مضادة للاكسدة جيدة . ظهر المعقد Pd-BAE كمضاد قوي للالتهاب عند تقييمه في التئام الجروح مبيناً "فعالية كبيرة لعلاج الحروق والجروح والتي استغرقت 9 ايام للشفاء في حين ان عقار سلفاديازين الفضة كمعيار يستغرق 16 يوم وبدون معالجة 18 يوم . اخيراً تم تقييم التأثير السمي لمعقد Co-BAE ضد خط خلايا سرطان القولون CaCo2 باستخدام فحص MTT للكشف عن امكانية المعقد كمضاد للسرطان مع IC50 109.1 mg ml^{-1} بالمقارنة مع خط الخلايا الطبيعي (WRL68).

Introduction:

Azo compounds play a vital role in technological advancement, healthcare improvement, and industrial sustainability. Their versatility guarantees their ongoing importance in scientific study and innovation [1]. Their importance stems from diverse chemical properties and a wide range of applications in many disciplines. With their durability, vibrant colors, and ability to change, azo compounds are indispensable in both industries and medicine [2, 3]. Azo compounds are commonly used in the production of synthetic colors for textiles, food, and cosmetics. Their stability and colour range make them valuable in the dyeing industry [4,5]. Furthermore, azo chemicals are used to generate drugs with antibacterial, anti-inflammatory, and anticancer properties. Structural modifications of these compounds can influence specific biological processes [6-8]. They are also used to colour polymers and make complex materials with distinct optical properties [9]. Azo compounds operate as intermediaries and catalysts in a wide range of industrial processes, improving the efficiency of chemical reactions such as the spectroscopic detection of metal ions in trace concentrations [10,11]. Recently, heterocyclic azo compounds have been utilised to create photochromic materials and sensors that detect light, temperature, and pH [12]. Furthermore, they promote sustainable practices by developing environmentally friendly azo-based materials [13, 14]. The aim of the study is a synthesis of a new ligand and its complexes with Co(II),Cu(II),Ag(I),Pd(II), and Pt(IV) derived from Enprofylline. Characterization of the synthesized compounds using elemental analysis, spectroscopy, and thermal analysis. Also evaluation of new compounds as antibacterial, anti-inflammatory, antioxidant, and anticancer agents.

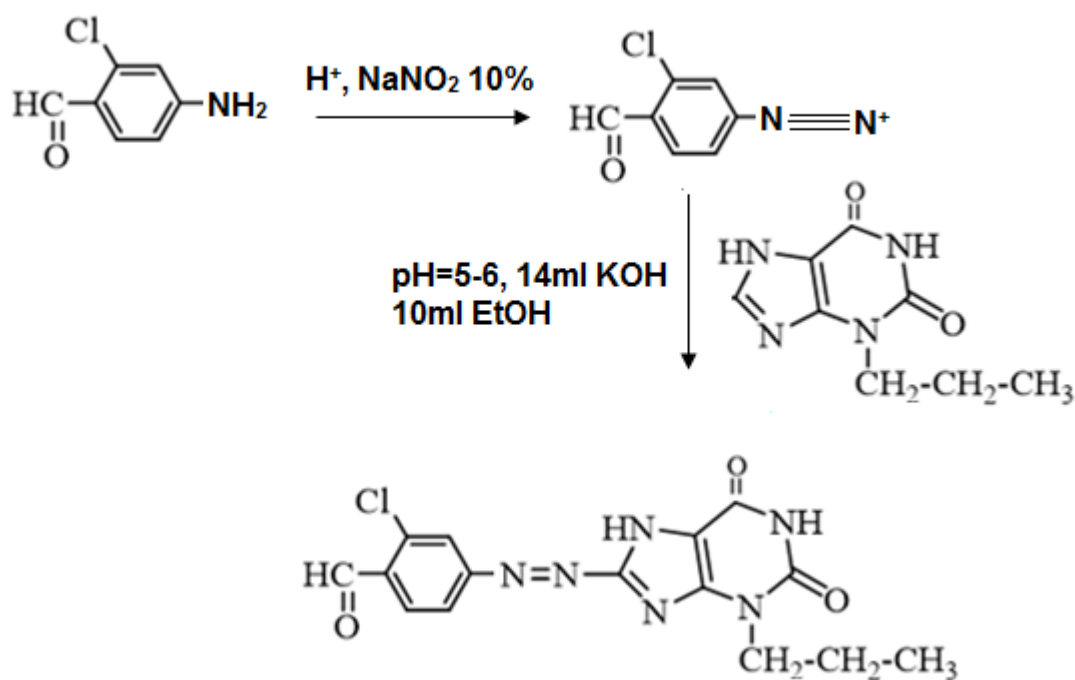
Experimental Part**Instruments and Materials**

All solvents and reagents, with high purity, were supplied from Sigma Aldrich and Fluka. UV-Vis spectra were recorded in ethanol using a Shimadzu UV-160A ultraviolet-visible

spectrophotometer. A Shimadzu FTIR-8400s Fourier Transform Infrared spectrophotometer ($200\text{--}4000$) cm^{-1} was used to record FTIR spectra using CsI discs. Thermal Analysis measures TG and DSC were carried out using a (Mettler) Thermogravimetric Analyzer, (C.H.N) Analysis, and Melting Point using Sturat Melting Point Apparatus. The ^1H NMR spectra were obtained on a (^1H NMR Spectrometer 4000 MHz

Synthesis of ligand [BAE]

The ligand [4-((2,6-dioxo-3-propyl-2,3,4,5,6,7-hexahydro-1H-purin-8-yl)diazenyl)benzaldehyde] [BAE] was synthesized following a modified procedure based on the literature, as illustrated in scheme (1) [15]. The diazonium salt was prepared by the reaction of (0.01 mole; 1.55 gm) for 4-amino-2-chlorobenzaldehyde as a primary amine with (0.01 mole; 1.94 gm) of Enprofylline as a coupling. The resulting azo product was isolated by filtration and washed with (1:1)[EtOH:H₂O] and then dried.



Scheme 1: A synthesis path of the ligand BAE

All complexes were synthesized in distilled water as a solvent with a mole ratio of (M: L) (1:2) by dissolving (2mmol, 0.7215g) of ligands (BAE) [4-((2,6-dioxo-3-propyl-2,3,4,5,6,7-hexahydro-1H-purin-8-yl)diazenyl)benzaldehyde]. The aqueous ligand solution was gradually added with stirring to an aqueous solution containing 1 mmol of the selected metals salts (AgNO_3 , CuCl_2 , CoCl_2 , $\text{PtCl}_4 \cdot 6\text{H}_2\text{O}$, $\text{PdCl}_2 \cdot \text{H}_2\text{O}$) at room temperature. Colored products formed, which were filtered, washed several times with a (1: 1) (H_2O :EtOH), and then dried. The suggested structures as appeared in Diagram 1

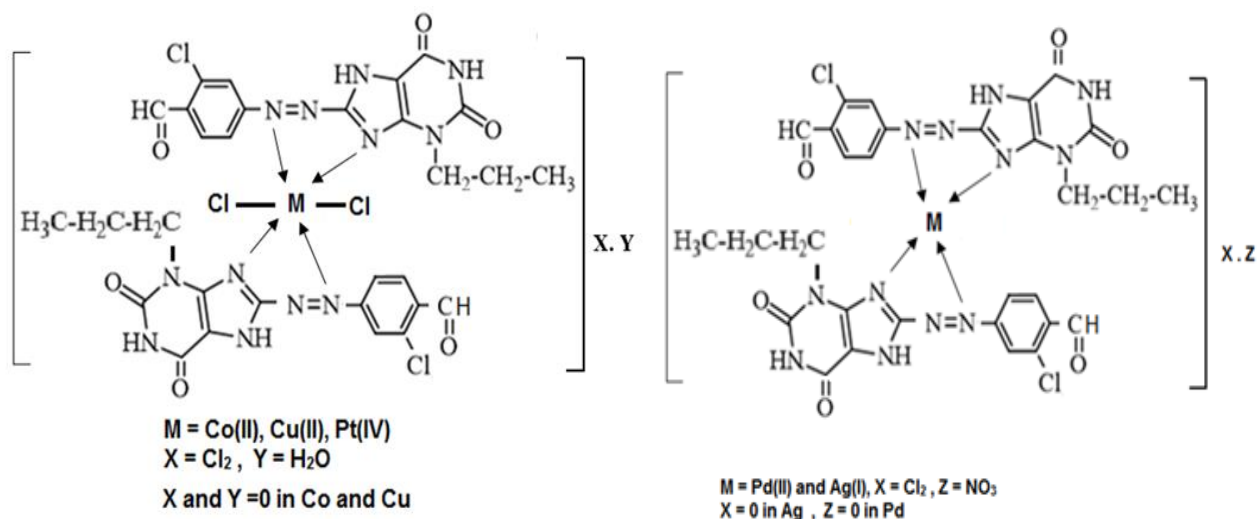


Diagram 1: Suggested structures of the BAE-Complexes

Antibacterial capacity performance

The biological activity of the ligand [BAE] and its complexes was evaluated against two bacterial strains: *Escherichia coli* (Gram negative ATCC: 25922) and *Staphylococcus aureus* (Gram positive ATCC: 25923). Discs were impregnated with 5mm of ($1 \times 10^{-3} \text{M}$) of BAE ligand and its complexes, the disc was left for fifteen minutes to disperse on the medium, and then it was incubated at (37 C°) for twenty-four hours to check the inhibition activity of specified bacteria on the BAE ligand and its complexes [16].

Assessment of Anti-oxidant Activity *in vitro*

a-Reductive ability

The reductive ability was evaluated using the method described in the literature [12], using 1 ml of each concentration of $[\text{Cu}(\text{BAE})_2\text{Cl}_2]$ Complex (0.02, 0.04, 0.08, 0.16, 0.32, and 0.64 mg/ml). Absorptivity was measured at 700nm. A Trolox solution (standard) was prepared as the standard following the same procedure. All experiments were conducted in duplicate.

b-DPPH Radical

Scavenging Activity Using the procedure outlined in the literature[17], the antioxidant activity of $[\text{Pt}(\text{BAE})_2\text{Cl}_2]\text{Cl}_2 \cdot \text{H}_2\text{O}$ and standard (vitamin C) was assessed depending on the radical scavenging activity of the stable DPPH free radical. After incubating at 37°C for 30 minutes, 3.9 ml of DPPH solution was mixed with an aliquot of extract or standard (0.625, 0.125, 0.250, and 0.500 mg/ml). The absorbance of each solution was then measured at 517 nm by spectrophotometer. Three duplicates of each measurement were conducted.

Anticancer activity

The MTT assay was used to evaluate the cytotoxic effects of $[\text{Co}(\text{BAE})_2\text{Cl}_2]$ at various concentrations various concentrations (6.2, 12.5, 25, 50, 100, 200, and $400 \mu\text{g/ml}$) adsorbed on ready-to-use spinal cords, as well as 400g/ml of the control cancer cell line (CACO-2) and normal cells (WRL-68) for comparison. Tumor cells (1×10^4 - 1×10^6 cells/ml) were grown in 96 flat-bottom micro-titer plates with a total capacity of 200 L of complete culture media in each well. The microplate was wrapped in sterile parafilm and shaken lightly. Plates were incubated for 24 hours at 37°C and 5% CO_2 . ELISA reader was employed to measure at a wavelength of 575 nm. The drug concentration required to achieve a 50% reduction in cell viability was determined through statistical analysis of the optical density measurements.

Result and Discussion

Scheme (1) illustrates the ligand (BAE) synthesis process, which involves diazotizing [4-amino-2-chlorobenzaldehyde] at (0-5)^oC to prevent the diazonium salt from disintegrating. This intermediate is then reacts with an alcoholic alkaline solution of the nucleophile enprofylline reacting with the selected ions [Co(II),Cu(II),Pd(II), Ag(I) and Pt(IV)] with the organized ligand (BAE) in [1:2] [M:L] mole ratio .As a neutral N,N-bidentate, the ligand functions.[C.H.N.] provided the physical characteristics and results, and Table (1) lists the metal percentage and chloride content for the structured compounds using the Mohr technique. They accord well with those that the proposed equations called for. Additionally, the synthesized compound's formulae were proposed based on data from molar conductivity, magnetic susceptibility, and spectral examinations. Every synthetic chemical dissolves in water. The molar conductance of all complexes was determined in deionized water at a concentration of 10⁻³ M, with the results summarized in Table 1. Complexes of Cu-BAE and Co-BAE were nonelectrolytes. Pt-BAE and Pd-BAE complexes, which were electrolyte(1:2) with chloride ion as a counter ion, but Ag-BAE complex has (1:1) electrolyte properties with NO₃⁻ as a counter ion [18]

Table1:Physical properties and elemental analyses data

No	Compounds (M.wt) (gm/mol)	M:L	Color λ (nm)	% Experimental (Theoretical)%					
				C%	H%	N%	M%	Cl%	Λ_m (S.mol ⁻¹ .cm ²)
1	BAE (C₁₅H₁₃N₆O₃Cl) 360.5	---	yellow 425	49.89 (49.93)	4.43 (3.60)	23.28 (23.30)	---	---	
2	[Ag(C₃₀H₂₆N₁₂O₆Cl₂)]NO₃ 890.87	1:2	pink 530	39.83 (40.40)	3.36 (2.91)	19.12 (18.85)	11.33 (12.10)	---	100
3	[Cu(C₃₀H₂₆N₁₂O₆ Cl₂)Cl₂] 856.74	1:2	green 569	41.56 (42.01)	3.49 (3.03)	19.35 (19.60)	6.61 (7.42)	16.17 16.57	26.2
4	[Co(C₃₀H₂₆N₁₂O₆ Cl₂)Cl₂] 850.9	1:2	orange 450	41.49 (42.31)	3.51 (3.05)	18.43 (19.74)	6.41 (6.92)	16.33 (16.68)	19.9
5	[Pt(C₃₀H₂₆N₁₂O₆Cl₂)Cl₂]. H₂O 1076.09	1:2	green 590	32.67 (33.45)	2.81 (2.41)	14.78 (15.61)	17.76 (18.13)	18.97 (19.79)	284
6	[Pd(C₃₀H₂₆N₁₂O₆ Cl₂)Cl₂] 898.4	1:2	green 618	39.53 (40.07)	3.33 (2.89)	17.51 (18.69)	11.09 (11.84)	14.39 (15.81)	300

Nature of complexes

The mole ratio method is the most commonly used technique to accurately determine the molecular formula of a metal complex in solution by estimating the metal ion to BAE[M:BAE] ratio. The mole ratio of [1:2][M:L] for all produced complexes was displayed in Figure (1) [1]

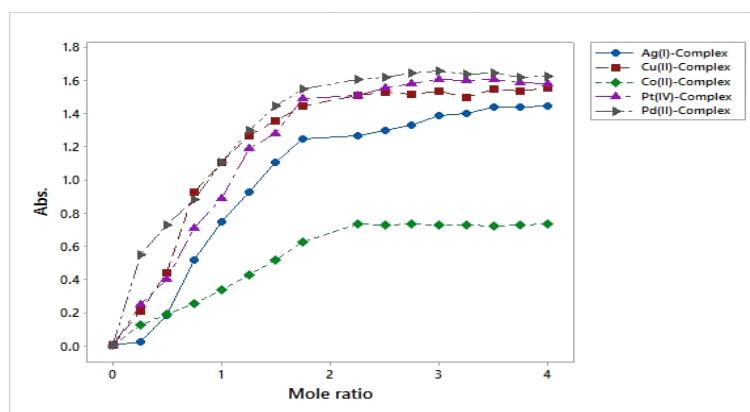


Figure 1: A Graph of mole ratio for BAE-Complexes

Stability Constant and Gibbs Free Energy of Complexes

The stability constant (K) has been calculated for all complexes using the equation below [20].

$$K = \frac{(1-\alpha)}{4 \alpha^3 C^2}$$

$$\alpha = \frac{Am - As}{Am}$$

Where

α = The degree of dissociation refers to the fraction of a mole for the reactant that undergoes dissociation.

As = The absorption of a complex (metal and ligand) as stoichiometric amounts

Am = The absorption of ligand excess solution.

C = The concentration (mole/l)

By applying the above equations and calculating (ln K), we conclude that the synthesized complexes have high stability, as it increases in the following order:

$[Pd(BAE)_2] Cl_2$ (13.579) > $[Cu(BAE)_2Cl_2]$ (13.067) > $[Pt(BAE)_2Cl_2]Cl_2.H_2O$ (13.020) > $[Co(BAE)_2Cl_2]$ (12.762) > $[Ag(BAE)_2]NO_3$ (12.465)

The Gibbs free energy (ΔG), was computed by utilizing the equation below [21].

$$\Delta G = -R T \ln K$$

Where:

T = (298°C) Absolute temperature in Kelvin

R = gas constant = 8.314 J.mol⁻¹.K.

Based on our data for calculating the (ΔG) of all complexes, the preparations are considered spontaneous. The following order represents values of (ΔG) and stability of complexes:

$[Ag(BAE)_2]NO_3$ (-3088.293) < $[Co(BAE)_2Cl_2]$ (-3161.877) < $[Pt(BAE)_2Cl_2]Cl_2.H_2O$ (-3225.798) < $[Cu(BAE)_2Cl_2]$ (-3237.443) < $[Pd(BAE)_2] Cl_2$ (-3364.295) J.mole⁻¹

Thermal Analysis (TGA) and (DSC)

Thermal degradation of BAE ligand and its complexes were assessed by (TGA) and (DSC) in the range (25-1000)C° in argon [Table (2)]. To validate the suggested structure and investigate the thermal degradation of BAE ligand and its complexes, thermal analyses were carried out. Additionally, lattice water molecules in $[Pt(BAE)Cl_2]Cl_2.2H_2O$ complex were lost in the first step at the ranges (25-130) C° is anticipated [22]. The findings seemed to be in good agreement with the formula that the analytical data had suggested [23]. According to the ligand (BAE) and its complexes' TGA curves, the thermal stability declines in the following order. Analysis of the (TGA) curves for the ligand (BAE) and its complexes indicates that their thermal stability decreases in the following order:

BAE(18.32%) < Pd-BAE(21.46%) < Ag-BAE(31.19%) < Pt-BAE(34.06%) < Cu-BAE(34.21%) < Co-BAE(36.28%)

Table 2 :(TGA - DSC) Data of the ligand (BAE) and its Complexes

Synthesized compound	Molecular Formula M.Wt. (g/mol)	Stage	TG. Extent of thermal fractionation on (°C)	Proposed part	Mass lack %		DSC. C°
					Calculate %	Found %	
BAE	BAE(C₁₅H₁₃N₆O₃Cl) 360.5	1	25-140°C	C ₆ H ₂	20.52	20.73	216.24°C exo 415°C exo
		2	140-300°C	C ₅ H ₁₁	19.14	19.7	
		3	300-1000°C	C ₄ N ₅ Cl	42.40	41.82	
		Residue	1000°C>	NO ₃	17.19	18.32	
[Ag(BAE) ₂]NO ₃	[Ag(C₃₀H₂₆N₁₂O₆Cl₂) NO₃ 890.87	1	140-200°C	C ₃ H ₃	4.37	4.85	382.60°C endo
		2	300-400°C	C ₅ H ₁₆ Cl ₂	16.50	16.58	
		3	650-800°C	C ₁₅ NH ₇	22.56	22.84	
		4	1000°C	C ₇ N ₁₀	25.14	24.53	
		Residue	>1000°C	AgO ₉ N ₂	31.41	31.19	
[Cu(BAE) ₂]Cl ₂	[Cu(C₃₀H₂₆N₁₂O₆Cl₂) Cl₂ 855.54	1	25-175°C	C ₂ HCl	7.06	7.05	216.89°C exo
		2	400-550°C	C ₈ H ₂₅ Cl ₃	26.55	26.54	308.80°C endo
		3	1000°C	C ₂₀ N ₂	31.28	32.15	
		Residue	>1000°C	CuN ₁₀ O ₆	34.98	34.21	
[Co(BAE) ₂]Cl ₂	[Co(C₃₀H₂₆N₁₂O₆ Cl₂)Cl₂ 850.9	1	25-175°C	C ₂ H ₁₀	3.99	4.12	239.49°C exo
		2	200-300°C	C ₂ H ₁₂ Cl ₂	12.57	12.67	249.67°C endo
		3	800-820°C	C ₁₇ H ₄ Cl ₂	32.78	32.76	
		4	1000°C	C ₉ N	14.33	14.19	
		Residue	>1000°C	CoN ₁₁ O ₆	36.30	36.28	
[Pt(BAE) ₂]Cl ₂ ·2H ₂ O	[Pt(C₃₀H₂₆N₁₂O₆Cl₂)Cl₂· 2H₂O 1076.09	1	25-130°C	C ₂ H ₆ Cl	6.08	6.151	232.74°C exo
		2	200-320°C	C ₂ Cl ₃	12.11	12.17	249.39°C endo
		3	1000°C	C ₂₆ H ₂₂ N ₇ Cl ₂	46.70	47.62	
		Residue	>1000°C	PtN ₅ O ₆	33.53	34.06	
[Pd(BAE) ₂]Cl ₂	[Pd(C₃₀H₂₆N₁₂O₆ Cl₂)Cl₂ 898.4	1	25-200°C	C ₂ H ₁₁ Cl	7.84	7.91	131.09°C exo
		2	400-550°C	C ₁₅ H ₁₀ Cl ₃	33.00	33.04	227.18°C endo
		3	1000°C	C ₁₃ H ₄ N ₁₂	36.50	37.51	
		Residue	>1000°C	Pd O ₆	22.53	21.46	

Electronic spectroscopy survey

Table (3) shows that the ligand (BAE) exhibits two bands: the first at 425 nm; 23589 cm⁻¹, and the second at 270 nm; 37037 cm⁻¹. These bands were ascribed to the (n→π*) transition of the intramolecular charge transfer (intra CT) that occurs via the carbonyl and azo moieties. The intramolecular transition [intra CT] for pyrimidine, imidazole, and benzene moieties was also restored for the second band in the UV area [24]

The electronic spectrum of diamagnetic(d^6) $[\text{Pt}(\text{BAE})_2\text{Cl}_2]\text{Cl}_2\cdot\text{H}_2\text{O}$ was clarified band at (1007nm; 9930 cm^{-1}) that assigned to $[^1\text{A}_{1g} \rightarrow ^1\text{T}_{1g}]$ transition. At the same time, the $[^1\text{A}_{1g} \rightarrow ^1\text{T}_{2g}]$ transition was observed at (780nm, 12820 cm^{-1}). The $[^1\text{A}_{1g} \rightarrow ^3\text{T}_{1g}]$ transition is obscured by the CT transition due to interference.

Also, this transition is weak or hidden due to geometrical distortion.

This is within octahedral geometry[25].

The electronic spectrum of (d^9) $[\text{Cu}(\text{BAE})_2\text{Cl}_2]$ complex was demonstrated (d-d). The transition bands at (1043nm; 95877 cm^{-1}), (903nm; 11074 cm^{-1}) and (569 nm; 16778 cm^{-1}) attributed to $[^2\text{B}_{1g} \rightarrow ^2\text{A}_{1g}]$, $[^2\text{B}_{1g} \rightarrow ^2\text{B}_{2g}]$ and CT transition respectively. The $^2\text{B}_{1g} \rightarrow ^2\text{E}_g$ transition is hidden within CT transition, consistent with Jahn-Teller effects and paramagnetic behavior [26]. The spectrum of (d^7) $[\text{Co}(\text{BAE})_2\text{Cl}_2]$ complex, has $\nu_1 = [^4\text{T}_{1g}(\text{F}) \rightarrow ^4\text{T}_{2g}(\text{F})]$ and $\nu_2 = [^4\text{T}_{1g}(\text{F}) \rightarrow ^4\text{A}_{2g}(\text{F})]$ were shown at (907nm; 11025 cm^{-1}) and (450nm; 22222 cm^{-1}). The $\nu_3 = [^4\text{T}_{1g}(\text{F}) \rightarrow ^4\text{T}_{1g}(\text{P})]$ was mixed with the (CT) transition [12], and diamagnetic property $[\text{Pd}(\text{BAE})_2\text{Cl}_2]$ complex appeared transitions that belong to $[^1\text{A}_{1g} \rightarrow ^1\text{A}_{2g}]$ transition at (915nm, 10900 cm^{-1}). As for the transition $[^1\text{A}_{1g} \rightarrow ^1\text{E}_{1g}]$ is so very weak and therefore is hidden within a double band at (618nm) which is assigned to (CT), [26].

Table 3 :Electronic transition, geometry and magnetic property of BAE ligand and its complexes at (10^{-4}M)

Compound	Wave length (nm)	Wave number (cm^{-1})	Assignment	Geometry	Magnetic property B.M.	
					Theor.	Exp.
BAE	270 425	37037 23529	$\pi \rightarrow \pi^*$ $n \rightarrow \pi^*$	\rightarrow --- \rightarrow	---	---
$[\text{Ag}(\text{BAE})_2]\text{NO}_3$	530	18867	CT	Tetrahedral	1.70	1.65
$[\text{Cu}(\text{BAE})_2\text{Cl}_2]$	1043 903 569	95877 11074 17574	$^2\text{B}_{1g} \rightarrow ^2\text{A}_{1g}$ $^2\text{B}_{1g} \rightarrow \text{B}_{2g}^2$ CT	Tetragonal	1.75	1.82
$[\text{Co}(\text{BAE})_2\text{Cl}_2]$	907 770 450	11025 12987 22222	$^4\text{T}_{1g}(\text{F}) \rightarrow ^4\text{T}_{2g}(\text{F})$ $^4\text{T}_{1g}(\text{F}) \rightarrow ^4\text{A}_{2g}$ (F) CT	Octahedral	3.82	3.86
$[\text{Pt}(\text{BAE})_2\text{Cl}_2]\text{Cl}_2\cdot\text{H}_2\text{O}$	1007 700 590	9930 14285 16949	$\text{A}_{1g} \rightarrow ^1\text{T}_{1g}$ $\text{A}_{1g} \rightarrow ^1\text{T}_{2g}$ CT	Octahedral	Dia	Dia
$[\text{Pd}(\text{BAE})_2]\text{Cl}_2$	915 618	10900 16181	$[^1\text{A}_{1g} \rightarrow ^1\text{A}_{2g}]$ CT	Square planar	Dia	Dia

$^1\text{HNMR}$ Spectra

The $^1\text{HNMR}$ spectra of the synthesized ligand and its complexes with the free ligand using TMS as standard and $\text{DMSO}-d_6$ as a solvent.

The BAE ligand exhibited two singlet signals at 12.18 ppm and 8.03 ppm, assigned to the NHimd (1H) and NHprm (1H) protons, respectively. A broad signal at (9.85)ppm was backed to the proton of the aldehyde [27]. There are multiple signals were shown at (7.37-7.0)ppm references to the benzene ring [17]. Table (4) presents all data on the ligand and its complexes. A slight change was found in the chemical displacement of the protons in the spectra of the complexes compared to the spectrum of the ligand (BAE)

Table 4 : ^1H NMR signals of BAE and its Complexes

Compound	$^1\text{H}, \text{NH}_{\text{imd}}$	$^1\text{H}, \text{NH}_{\text{prm}}$	$^1\text{H}, \text{CHO}$	CH_3	CH_2	Benzene	H_{prm}
BAE	12.18	8.03	9.85	2.99	3.81	7.37-7	3.90
$[\text{Ag}(\text{BAE})_2] \text{NO}_3$	12.16	8.0	9.82	2.95	3.79	7.21-7.1	3.88
$[\text{Pt}(\text{BAE})_2\text{Cl}_2]\text{Cl}_2 \cdot \text{H}_2\text{O}$	14.42	7.39	9.69	2.35	3.71	7.29-7.1	3.77
$[\text{Pd}(\text{BAE})_2] \text{Cl}_2$	12.12	8.08	9.87	3.01	3.83	7.30-6.9	3.92

FTIR Spectra

The FT-IR spectrum of the BAE ligand was compared with those of the synthesized metal ion complexes. The spectra of the complexes displayed absorption bands corresponding to those of ligands with various variations as a result of the chelating. Using a CsI disk, the most significant vibrations were observed in the $250\text{--}4000 \text{ cm}^{-1}$ range. The $\nu(\text{NH})$ of the imidazole and pyrimidine moieties caused a triplet band to appear at $(3429, 3344, \text{ and } 3230) \text{ cm}^{-1}$ in the spectra of the BAE ligand [Figure 18] [28]. This band remained without change in the complexes spectra Figures[16-21], indicating that there was no chelating through this moiety. The little change in shape and position for this triplet band, was presumably according to changes in sharpness. The spectrum of (BAE) was showed a doublet band at $(1560, 1598) \text{ cm}^{-1}$ which was referred to stretching imine of imidazole ring for Enprofylline, change in profile and position of this band because of complexation with the metal ion[29,30]. The band referred to $\nu(\text{C}=\text{O})$ of pyrimidine ring in Enprofylline was exhibited at $(1647) \text{ cm}^{-1}$ in the spectrum for the ligand(BAE) there was a slight change in this band in the spectra of the complexes when compared with the spectrum of ligand, which indicates that the carbonyl group was not within the coordination sphere. The selection bands $\nu(\text{N}=\text{N})$ and $\nu(\text{C}-\text{N}=\text{N}-\text{C})$ for the azo compounds appeared at $(1461, 1411) \text{ cm}^{-1}$ and $(1257) \text{ cm}^{-1}$ in(BAE) spectrum. These bands showed a reduction in position and intensity in complex spectra due to complexation. Addition bands were observed in the spectra of the complexes, due to the binding of metal ions with the ligand(BAE). [Table5][31]

Table 5 : FTIR bands of BAE ligand and it Complexes

Com.	$\nu(\text{NH})$	$\nu(\text{C}=\text{O})$	$\nu(\text{C}=\text{N})$	$\nu(\text{N}=\text{N})$	$\nu(-\text{C}-\text{N}=\text{N}-\text{C}-)$	$\nu(\text{M}-\text{N})_{\text{imd}}$	$\nu(\text{M}-\text{N})_{\text{azo}}$	$\nu(\text{M}-\text{Cl})$
BAE	3429 3344 t 3230	1647			1257sh,st.	-	-	-
$[\text{Ag}(\text{BAE})_2]\text{NO}_3$	3433br.		1556		1242w.	685	534	-
$[\text{Cu}(\text{BAE})_2\text{Cl}_2]$	3350m	1600	1602	1471b.	1240sh.	685	518	318
$[\text{Co}(\text{BAE})_2\text{Cl}_2]$	3343s.	1650 1600	1508 1461		1186sh.	675	522	416
$[\text{Pt}(\text{BAE})_2\text{Cl}_2]\text{Cl}_2 \cdot \text{H}_2\text{O}$	3350	1641vw	1508 1461	1388 1413	1255m.	681	536	416
$[\text{Pd}(\text{BAE})_2] \text{Cl}_2$	3342	1640vw	1506 (vw)	1461m.	1254s.	682	526	435

st=strong, m=medium, w=weak, vw=very weak, d=doublet and t=triplet

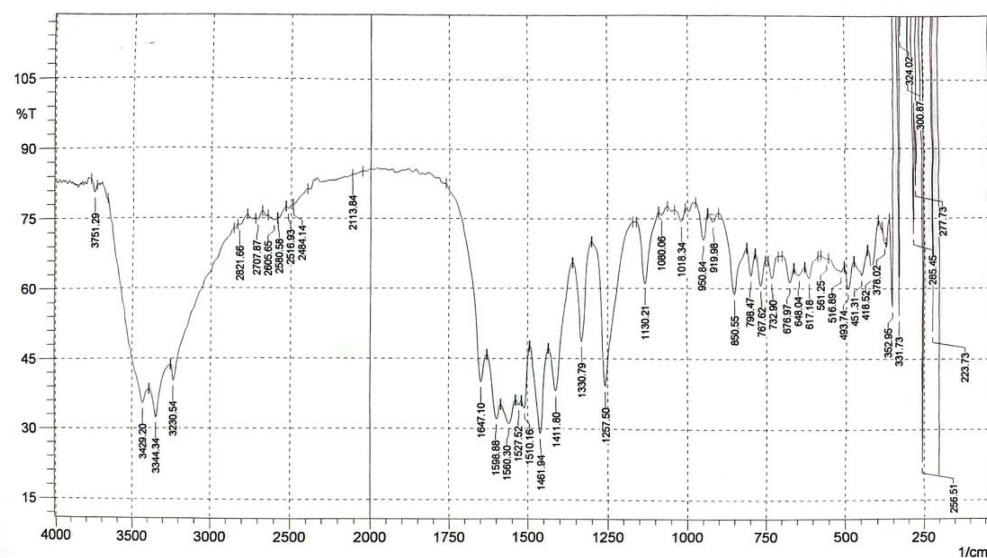


Figure 2: FTIR spectrum of BAE ligand

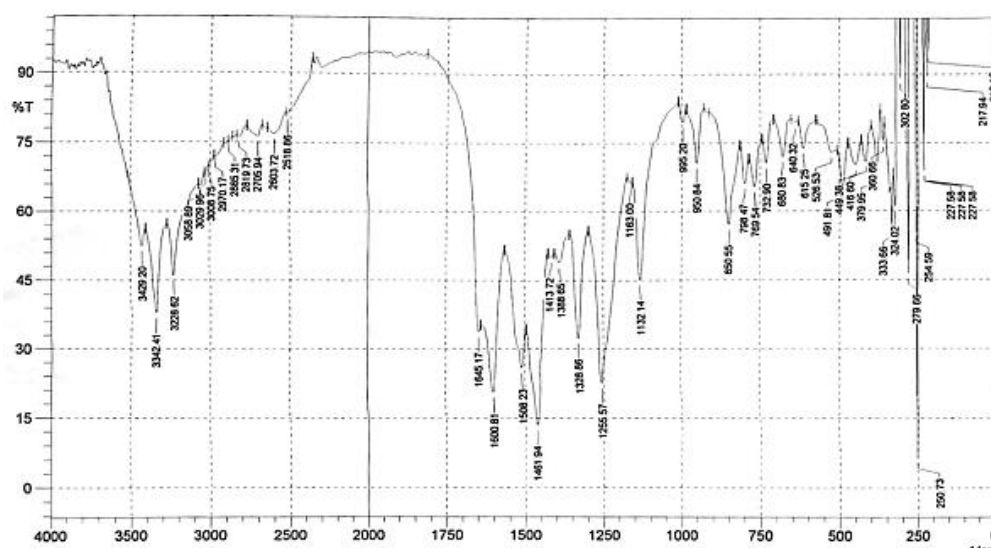


Figure 3: FTIR spectrum of $[Pt (BAE)_2Cl_2]Cl_2.H_2O$ Complex.

Deactivation capacity Antibacterial

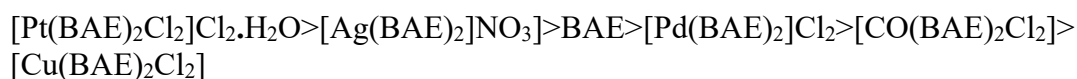
Staphylococcus aureus (Gram-positive) and *Escherichia coli* (Gram-negative) were the two chosen bacterial species against which the biological activity of the ligand (BAE) and its complexes were investigated. The solution concentration was 10^{-3} mole, and water was used as the solvent. Its efficacy was assessed in comparison to the synthesized compounds, employing amoxicillin as a reference standard. The disc's surrounding zone of inhibition of bacterial growth was managed. Table 6 lists the ligands' (BAE) and their complex's deactivation capacity against the bacterium switch. According to the study's findings, they had varying capacities to deactivate the two types of chosen bacteria, as detailed below:

The results showed different deactivating capacities against *Escherichia Coli* and *Staphylococcus aureus* as explained below:-

For *Escherichia Coli*:-

$[Pd(BAE)_2]Cl_2 > [Co(BAE)_2Cl_2] > [Ag(BAE)_2]NO_3 > [Cu(BAE)_2Cl_2] > [Pt(BAE)_2Cl_2]Cl_2.H_2O > BAE$.

For *Staphylococcus aureus*:-



The activity of the metal complexes seemed to be higher. The observed effect is attributed to enhanced lipophilicity, as rationalized by Tweedy's chelation theory and Overtone's concept. The variables that were considered to limit antibacterial activity when cell permeability and lipid membranes that favor the crossing of only lipid-soluble material because of liposolubility. Over time, the ligand orbital will partially share the metal ion's positive charge with the chelating moiety, reducing the metal's polarity to a higher degree upon coordination [31,32].

Table 6 : Antibacterial capacity of synthesized compounds

Synthesized Compounds	Gram(-) Negative	Gram(+) Positive
	<i>Escherichia Coli (E-Coli)</i>	<i>Staphylococcus aureus</i>
Amoxicillin	15.0	20.0
1 [Ag(BAE) ₂]NO ₃	23.0	24.0
2 [Cu(BAE) ₂]Cl ₂	21.5	17.5
3 [Co(BAE) ₂]Cl ₂	23.5	18.5
4 [Pt(BAE) ₂]Cl ₂ ·H ₂ O	21.0	25.5
5 [Pd(BAE) ₂]Cl ₂	25.5	18.8
6 BAE	16.0	20.0

Anti-inflammatory effectiveness

Efficiency in reducing inflammation [Pd(BAE)₂]Cl₂ at (1.5mM), silver sulfadiazine (positive control), and negative control were tested for their capacity to cure burns by measuring the number of days needed to recover. According to the data, burns could be healed in 9 days with the [Pd(BAE)₂]Cl₂ complex as opposed to 16 and 18 days with silver sulfadiazine and the negative control, respectively. In certain complexes, the presence of the Enpropyline heterocyclic ring with a strong anti-inflammatory effect as well as effective moieties on the benzene and naphthalene rings is the primary cause of the increased anti-inflammatory action [2,6].

Anti-oxidant properties

In vitro antioxidant assessment was done by two methods. The first method is a radical scavenging method utilizing DPPH (1,1-diphenyl-2-picrylhydrazyl) on [Pt(BAE)₂]Cl₂·H₂O complex with vitamin (C) as a control [33]. Table 7 showed that the data of DPPH radical scavenging activity, it was noted that the [Pt(BAE)₂]Cl₂·H₂O complex has higher antioxidant activity than vitamin (C) for all selected concentrations. As well as the second method is a reductive ability, which has been applied to [Cu(BAE)₂]Cl₂. Table 8 manifested absorbance of the complex and vitamin (E) as control, this data indicates that the complex has higher antioxidant effectiveness than vitamin (E).

Table 7: DPPH radical scavenging activity of [Pt(BAE)₂Cl₂]Cl₂.H₂O and Vitamin C

Concentration (Mg/ml)	DPPH Radical Scavenging Activity (Mean ± SD; %)	
	[Pt(BAE) ₂ Cl ₂]Cl ₂ .H ₂ O	Vitamin C
12.5	54.31± 1.802	39.66±2.52
25.0	60.28±4.723	41.33±10.01
50.0	67.88±5.930	48.33±8.50
100.0	70.79±5.354	53.00±10.53
200.0	78.61±3.204	65.01±11.73

Table 8 : Reductive Ability of [Cu(BAE)₂Cl₂] and Vitamin E

Concentration (Mg/ml)	Absorbance of Reductive Ability(Mean ± SD)	
	[Cu(BAE) ₂ Cl ₂]	Trolox(Vitamin E)
0.08	0.898± 0.001	0.108±0.001
0.16	0.909±0.003	0.114±0.004
0.32	1.09±0.003	0.132±0.007
0.64	1.493±0.006	0.211±0.015

Survey of cancer Effectiveness

A colon cancer cell line was used to assess the cytotoxic effect of [Co(BAE)₂Cl₂] utilizing 3-(dimethylthiazol-2-yl)-2,5-diphenyltetrazolium bromide (MTT) (CACO-2). The MTT assay was employed to evaluate cell viability and inhibition rate in the tumor cell line across varying concentrations of the complex. In comparison to the normal cell line WRL-68 (Figure 4), the percentage viability of treated cells was computed [34]. In the CACO-2 cell line, the cytotoxic effect of [Pd(BAE)₂]Cl₂ at concentrations ranging from 6.2 to 400 µg/ml showed a dose-dependent reduction in cell viability (Table 9). A metal ion binds to DNA at the (N7) locations of two guanine or guanine and adenine bases, preventing transcription and blocking DNA replication. The morphological characteristics of the complexes that cause cell death and DNA damage determine how effective they are at killing cancer cells. Additionally, it was discovered that the IC-50 values for the CACO-2 and WRL-68 cell lines were 160.3 and 105.9 µg/ml, respectively. This indicates a strong cytotoxic selectivity between cancerous and normal cell lines.

Table 9: Cytotoxicity effect of [Pd(BAE)₂]Cl₂ on CACO-2 and WRI-68 cells after incubation at 37°C for 24 hours

[Pd(BAE) ₂]Cl ₂ (µg/mL)	Viable cell count of CACO-2 cell line Mean± S.D.	Viable cell count of WRL-68 cell line Mean± S.D.
400.00	51.85 ± 1.48	79.21±1.92
200.00	63.23 ±2.99	84.45± 2.60
100.00	71.64 ±2.21	92.21± 0.47
50.00	85.92 ±4.14	95.33± 1.99
25.00	95.60 ± 0.76	95.80 ±2.68
12.50	92.55 ±6.44	94.29 ±2.98
6.25	95.60 ± 0.69	94.91 ±1.91

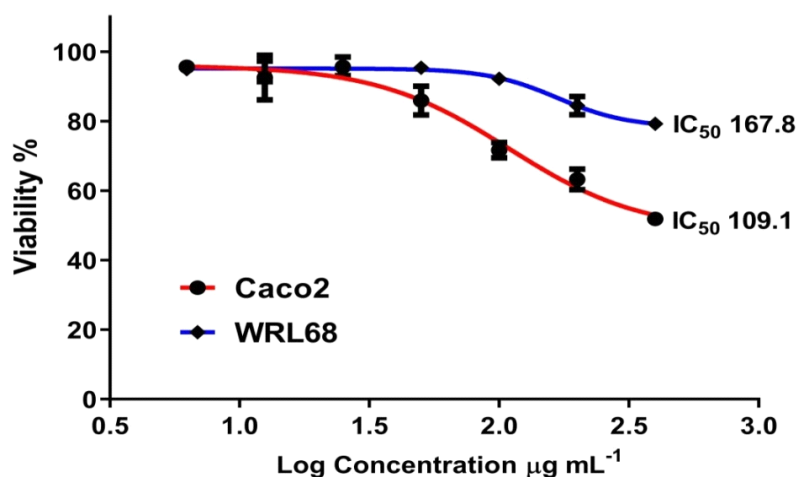


Figure 4 : Cytotoxic effect of $[\text{Co}(\text{BAE})_2\text{Cl}_2]$ on CACO-2 and WRL-68 cells after incubation for 24-hour at 37.

Conclusion

Analytical physicochemical analyses confirmed the successful synthesis of the new azo ligand BAE, formed by the coupling reaction of diazonium salt with enprofylline. The BAE ligand interacted with specified metal ions through the azo and imidazole nitrogen in the Enprofylline molecule, forming a pentagonal chelate ring and functioning as a neutral N,N-bidentate chelating ligand. The ligand and metal ions exhibit a binding interaction at specific coordination sites. The electronic, FTIR, and ¹HNMR spectra of complexes showed a significant shift compared to ligand. In contrast to the deformed octahedral (D_{4h}) of the Cu(II) complex, magnetic moment and electronic spectra data for compounds with an octahedral shape were proposed for [Co(II), Ag(I), Pt(IV) and Pd(II)] complexes. The antibacterial, antioxidant, anticancer properties and wound healing of the ligand and its complexes were evaluated, that approved all the synthesized compounds have good biological activity.

Acknowledgement

The authors would like to thank the University of Baghdad, the College of Science, Department of Chemistry for their support.

References :

- [1] I. T. Ives, A. M. Hu, and J. B. Wang "Colorimetric and Spectroscopic Studies of Metal Complexes: Advances and Applications", *Coordination Chemistry Reviews*, Vol.469,pp.214156, 2023.
- [2] Z. Z. Abd and A.K. Abbas, "Metal Complexes of Adenine Azo Ligand: Synthesis, Identification and Study some of their Applications", *Iraqi Journal of Science*, Vol.65 ,no.3,pp. 1212– 1229, 2024
- [3] N. Ertan and P. Gurkan, " Synthesis and properties of some azo pyridone dyes and their Cu(II) complexes", *Dyes and Pigments*, Vol. 33,pp. 137-147, 1997.
- [4] P. L. Garcia, R. M. Brown, and J. D. Zhao "Azo Dyes: Recent Advances and Future Directions in Research", *Dyes and Pigments*, Vol.216, pp.110675,2023.
- [5] J. P. Koster, M. H. Lee, and T. A. Davis "New Insights into the Colorimetric Properties of Transition Metal Complexes: Applications in Chemical Sensing and Imaging", *Chemical Society Reviews* Vol.52,no.5,pp.2123-2156,2023.
- [6] L. J. Roberts, M. K. Thompson, and H. R. Ali "Azo Compounds in Medicinal Chemistry: A Comprehensive Review of Their Biological Activities and Therapeutic Potential" *European Journal of Medicinal Chemistry*, Vol.227,pp.113893,2022.

- [7] A.K.Sharma, V.A. Singh and R.S. Patel, "Recent Advances in Azo Compounds: Biological Activities and Pharmaceutical Applications" *Bioorganic & Medicinal Chemistry*, Vol.45,no.7,pp.115678,2023.
- [8] P.M.Gomez, J.N. Lee and T.Y. Zhang,"The Role of Azo Compounds in Drug Discovery: Exploring Their Biological and Pharmacological Properties", *Journal of Medicinal Chemistry*, Vol.64,no.18,pp.13872-13888, 2021.
- [9] M.R. Hartmann and A.J. Smith, "Thompson, L.C.; Advancements in the Synthesis and Application of Colorimetric Metal Complexes", *Dalton Transactions*,Vol.48,no.32,pp. 11856-11867, 2019.
- [10] M.R. Jones, T.H. Lee, and K.C. Martinez, "Novel Ligand-Based Metal Complexes for Spectrophotometric Detection of Trace Metal Ions: Design, Synthesis, and Applications", *Journal of the American Chemical Society*,Vol.143,no.29,pp.11120-11131, 2021.
- [11] H. Liu, L. J. Zhang, and W. L. Chen, "Spectrophotometric detection of trace metal ions using metal complexes: Recent advances," *Talanta*, vol. 263, p. 124218, 2023
- [12] A. K. Abbas and W. W. AL-Qaysi, "Synthesis and characterization of novel nano azo compounds as a new pH sensor," *Arabian Journal for Science and Engineering*, vol. 48, no. 1, pp. 399–415, 2023.
- [13] L. N. Johnson, A. E. Brown, and C. M. Smith, "Recent advances in metal complexes for industrial and medical applications," *Journal of Industrial and Engineering Chemistry*, vol. 104, pp. 230–245, 2022
- [14] N. P. O'Connor, R. L. Patel, and E. H. Zhang, "Molecular design and applications of azo dye complexes in printing and optical devices," *Materials Science and Engineering: R: Reports*, vol. 134, pp. 32–50, 2019
- [15] H. A. K. Kyhoiesh and Kh. J. Al-Adilee, "Synthesis, spectral characterization, antimicrobial evaluation studies and cytotoxic activity of some transition metal complexes with tridentate (N,N,O) donor azo dye ligand," *Results in Chemistry*, vol. 3, no. 4, pp. 100245, 2021.
- [16] A. Y. Mohammed and L. S. Ahamed, "Synthesis of new substituted coumarin derivatives containing Schiff-base as potential antimicrobial and antioxidant agents," *International Journal of Drug Delivery Technology (IJDDT)*, vol. 12, no. 3, pp. 1279–1281, 2022.
- [17] A. A. Majeed and A. M. Noori Khaleel, "Evaluation of the anticancer and biological activity by new amide compound of trimethoprim with some of its complexes," *Caspian Journal of Environmental Sciences*, vol. 22, no. 1, pp. 9–22, 2024.
- [18] W. J. Geary, "The use of conductivity measurements in organic solvents for the characterization of coordination compounds," *Coordination Chemistry Reviews*, vol. 7, no. 1, pp. 81–122, 1971
- [19] D. A. Skoog, F. J. Holler, and S. R. Crouch, *Principles of Instrumental Analysis*, 7th ed. Boston, MA: Cengage Learning, 2017.
- [20] J. H. Lee, P. M. Johnson, and L. C. Evans, "Determination and application of stability constants for metal complexes in various chemical systems," *Journal of Chemical Thermodynamics*, vol. 126, pp. 150–162, 2018.
- [21] J. Zhang, C. Liu, and X. Zhou, "Gibbs free energy of formation of metal–organic frameworks: A comprehensive review," *Chemical Reviews*, vol. 117, no. 22, pp. 13354–13394, 2017.
- [22] T. Q. Manhee and A. J. Alabdali, "Synthesis, characterization and anticancer activity of Ni(II), Cu(II), Pd(II) and Au(III) complexes derived from novel Mannich base," *Vietnam Journal of Chemistry*, vol. 62, no. 2, pp. 201–210, 2024
- [23] C. A. Lewis, R. K. Smith, and J. L. Roberts, "Thermal analysis and stability of coordination complexes: Evidence from TG-DTG studies," *Journal of Thermal Analysis and Calorimetry*, vol. 143, no. 3, pp. 1067–1078, 2021.
- [24] R. K. Patel, S. H. Nguyen, and J. D. Lee, "Electronic spectra of azo compounds: Insights into charge transfer and π – π^* transitions," *Journal of Molecular Structure*, vol. 1338, p. 132678, 2023.
- [25] A. A. S. Al-Hamdani and R. G. Hamoodah, "Transition metal complexes with tridentate ligand: Preparation, spectroscopic characterization, thermal analysis and structural studies," *Baghdad Science Journal*, vol. 13, no. 4, pp. 770–781, 2016.
- [26] N. M. Mallikarjuna and J. Keshavayya, "Synthesis, spectroscopic characterization and pharmacological studies on novel sulfamethaxazole based azo dyes," *Journal of King Saud University – Science*, vol. 32, pp. 251–259, 2020

- [27] N. M. Aljamali, "Review in (NMR and UV-Vis) spectra," *International Journal of Medical Research and Pharmaceutical Sciences*, vol. 2, no. 1, pp. 28–36, 2015.
- [28] R. M. Silverstein, F. X. Webster, D. J. Kiemle, and D. L. Bryce, *Spectrometric Identification of Organic Compounds*, 8th ed. Hoboken, NJ: Wiley, 2023.
- [29] S. H. Mahdi and L. K. Abdul Karem, "Synthesis, characterization, anticancer and antimicrobial studies of metal nanoparticles derived from Schiff base complexes," *Inorg. Chem. Commun.*, vol. 165, pp. 112524, Jul. 2024.
- [30] N. M. Abdalsahib and L. K. A. Karem, "Preparation, characterization, antioxidant and antibacterial studies of new metal (II) complexes with Schiff base for 3-amino-1-phenyl-2-pyrazoline-5-one," *Int. J. Drug Deliv. Technol.*, vol. 13, no. 1, pp. 290–296, 2023.
- [31] D. P. Mishra, P. K. Sahu, B. Acharya, S. P. Mishra, and S. Bhati, "A review of the synthesis and application of azo dyes and metal complexes for emerging antimicrobial therapies," *Results in Chemistry*, vol. 10, p. 101712, 2024.
- [32] L. S. Ahamed, "Synthesis of new five-membered heterocyclic compounds from 2-furfuryl mercaptan derivative and evaluation of their biological activity," *Journal of Global Pharma Technology*, vol. 10, no. 11, pp. 298–304, 2018.
- [33] S. H. Sherif and B. Gebreyohannes, "Synthesis, characterization, and antioxidant activities of genistein, biochanin A, and their analogues," *Journal of Chemistry*, vol. 2018, no. 2, pp. 1–6, 2018.
- [34] R. A. Ali, L. S. Ahamed, and Sh. I. Ch. Al-Khzraji, "Synthesis, characterization, and study of anticancer activities of new Schiff bases and 1,3-oxazepine containing drug," *Russian Journal of Bioorganic Chemistry*, vol. 50, pp. 28–33, 2024